IEEE Access
Multidisciplinary | Rapid Review | Open Access Journal

Received 29 June 2022, accepted 21 July 2022, date of publication 26 July 2022, date of current version 29 July 2022.

*Digital Object Identifier 10.1109/ACCESS.2022.3194069*

RESEARCH ARTICLE

# Automatic Rescheduling of Generator for Rotor Speed Regulation by KRASOVSKII's Theorem

**AMRENDRA KUMAR KARN[1], SALMAN HAMEED[1], (Senior Member, IEEE), MOHAMMAD SARFRAZ[1], (Member, IEEE), MOHD RIZWAN KHALID[1], (Member, IEEE), AND JONG-SUK RO[2,3], (Senior Member, IEEE)**

[1]Department of Electrical Engineering, Aligarh Muslim University, Aligarh 202002, India
[2]School of Electrical and Electronics Engineering, Chung-Ang University, Dongjak-gu, Seoul 06974, Republic of Korea
[3]Department of Intelligent Energy and Industry, Chung-Ang University, Dongjak-gu, Seoul 06974, Republic of Korea

Corresponding Author: Jong-Suk Ro (jongsukro@gmail.com)

This work was supported in part by the National Research Foundation of Korea (NRF) funded by the Korean Government (MSIT) under Grant NRF-2022R1A2C2004874; in part by the Korea Institute of Energy Technology Evaluation and Planning (KETEP); and in part by the Ministry of Trade, Industry & Energy (MOTIE) of the Republic of Korea under Grant 20214000000280.

**ABSTRACT** Emergency control of the power system is performed via generator rescheduling or load shedding depending upon the availability of generation and demand. This paper presents a generator rescheduling method based on Krasovskii's theorem for enhancing rotor speed regulation during multiple contingency conditions. The speed governor in automatic generation control (AGC) and automatic voltage regulator (AVR) are indispensable components of the control mechanism for deploying any control scheme. Contingencies may lead the security state of the power system towards a preventive, emergency, and restorative state. Generally, there is a violation of equality constraints of active and reactive power in the corrective security state. However, in this paper, the corrective security state considers a significant imbalance in active power with a generation capacity always greater than load. For rotor angle stability, active power delivery by the generator met the demands, whilst the turbine and automatic speed governor together balance it by changing the set point of the turbine inlet. This paper investigates the rotor stability by triggering a new set point by the rescheduling of the generator. The strategy proposed encompasses the broad domain of active power imbalance using Krasovskii's theorem, which is an extensive form of the Lyapunov stability theorem for the nonlinear multivariable autonomous system. The proposed control scheme is deployed on an IEEE-10 machine 39-bus system for validation and feasibility detection. It is found that the proposed scheme is more accurate than the conventional turbine automatic speed governor close loop system. Moreover, there is turbine power-saving up to 400 MW. In addition, the rotor attains steady-state speed quicker up to 5-10 sec and attains synchronous speed in all the cases considered, i.e., single load outage; multiple load outage; area outage; and load increment. The MATLAB® and the CVX platform are used to validate the proposed concept.

**INDEX TERMS** Generator rescheduling, power system contingency, security state, speed regulation.

## NOMENCLATURE

| | |
|---|---|
| *AVR* | Automatic voltage regulator |
| *AGC* | Automatic generation control |
| *PSS* | Power system stabilizer |
| *H* | Machine constant of generator |
| *M* | Angular momentum of generator |
| $E'_{qi}$ | Sub transient quadrature axis of the stator |
| $E'^{STEADY}_{qi}$ | Pre contingency equilibrium value of $E'_{qi}$ |
| $x'_{di}$ | Sub transient direct axis reactance of the generator |
| $x_{di}$ | Direct axis reactance of the generator |
| $E_{fi}$ | Rotor field voltage reference |
| $T_{doi}$ | The open axis time constant of the rotor field circuit |

The associate editor coordinating the review of this manuscript and approving it for publication was Sze Sing Lee.

| | |
|---|---|
| $\delta_{ij}$ | Angle difference between buses |
| $B_{ij}$ | Susceptance of reduced bus matrices between buses |
| $G_{ij}$ | Conductance of reduced bus matrices between buses |
| $P_{me}$ | Governor set pint input |
| $J$ (.) | Jacobean of matrices |
| $J$ (.)$^*$ | Transpose of Jacobean matrices |

## I. INTRODUCTION

The power system has a large intertwined connection among its elements like generator, load, bus, circuit breaker, and transmission line. there are many control section that manages active and reactive power flow like energy management systems and distribution management system to operate power supply in optimal and under safe margin. Great interconnected network from generation to load end. Different kinds of Contingency can draw power system security states among preventive, corrective, and emergent stages [1]. Generally, the transformer trappings, automatic voltage regulator (AVR), generator rescheduling, load curtailment, and FACTS devices cure the ill-health condition of the power system security state. When sections of a transmission line suffer from an outage, the remaining line is overloaded due to excessive power flow greater than the thermal and insulation limit of the line. If this condition persists for a long time then it causes more damage to the line transformer and generator. The automatic generation control (AGC) and AVR manage and control the terminal voltage and speed of the generator. The speed and active power are controlled by AGC controlling turbine set point and terminal and reactive power are governed by field current control of the generator by an AVR. An AVR has a very fast operating time but AGC has a slow dynamic due to various mechanical parts associated with it. During the prolonged effect of contingency, there is a rise in the condition of imbalance of active and reactive power delivered by generators and consumed by transmission sections and loads. Each generator is accompanied by AGC and AVR which are capable to maintain the speed, frequency, and voltage of the generator. Due to large operating time and generation rate constrain, the angular speed and the frequency of the generator varies during the transient time [2], [3]. Each generator has its maximum limit of active reactive power dispatch limit according to its design. In this paper, generator rescheduling is performed under a corrective security state.

Under a preventive security state, static security or inequality constraints for secure operation are violated, mainly line loading is threatened. Under a corrective security state, the equality constraint of active and reactive power is violated. Corrective security state comes due to large time adversarial effective of preventive state caused due to security measures carried by relay operation or due to sudden catastrophic effects like generator outage, load outage, etc. If there is a loss of excessive load, generation, or both, then the security state generally comes under a corrective state, and rescheduling the generator becomes an important and economical measure to prevent the wastage of turbine mechanical power. Power plants have some reserves like spinning, and hot reserves, to ensure and maintain the power supply when load demand and transmission loss exceed the generation [4], [5]. The power system must stand with all kinds of contingency, system all the voltages and frequency of buses should be brought under certain limits to prevent a blackout. In a corrective security state generator, rescheduling is performed when there is a generation surplus and load curtailment is performed when load demand exceeds the generation [6], [7].

Initially, the speed governor set point is determined for economic load dispatch. As active power of the generator is controlled in the feedback loop of the speed governor, turbine, and generator. So due to these mechanical components' large time constant, rotor speed fluctuates drastically under active power imbalance conditions and settles down after a large time than the AVR response. In the meantime post contingency, the rotor speed varies and hence the frequency of power supply is altered, and inter oscillation of rotor angle of the generator occurs. In most recent literature on generator rescheduling does not consider the AGC, AVR, and turbine operation that will not justify and comply with real-world applications. As per description and illustration in [3] and [8] turbine, speed governor, and power system stabilizer operation significantly affects the power system control and functioning. In this paper, the Authors resolve the abovementioned mismatch to fill the vacant space of research. This background of generator rescheduling and load curtailment under preventive and emergency security states has been a subject of research effort for a decade. It has been always challenging to resolve this issue on the computational and control deployment hand. The key concern of this paper emphasizes on comprehensive method of rotor angular stability by generator rescheduling. The focus is kept on the universal method of reallocation of power setpoint fed to the generators via turbine for improving the rotor speed in the time domain. Here in this paper generator rescheduling solution approach is performed for emergency security states. In this paper, four case studies are taken that encompass all relevant cases of generator rescheduling under an emergency security state.

The main objectives of the paper are:

- To study the effect of the generator rescheduling under emergency security contingency.
- To develop the self-healing, self-regulatory and automatic control strategy that performs well during the above mentioned issue.

## II. LITERATURE REVIEW AND RESEARCH GAP

The corrective action is a set of actions that is used to control irregularities occurred in the power system. It may be under a preventive security state or emergency security state. In the literature, an emergency security state is also termed as a corrective security state. As the frequency and speed of the synchronous machine are directly proportional, so increase in speed will cause frequency deviation. In [2] and [3], the

primary and secondary frequency control is presented with governor rate constrain and storage utilization, respectively. In [1], the IEEE-39 bus system is considered with four load frequency control areas and event-triggered based frequency control in the network is performed. In [4], the distributed model predictive control with generation rate and other constraints is performed.

In [5], the authors presented the technique of frequency stabilization by driving the operation of a power system stabilizer (PSS) in an intelligent framework. The wind turbine is always prone to variation in wind power. Due to the growing integration of wind power in a generation, in [6]–[9] the frequency regulation methodology is proposed based on the observation of deloading effect and variable frequency droop characteristic. The frequency regulation in distributed generation is presented in [10] by optimizing the control variable with particle swarm and gravity search algorithm. In [11], AGC performance is evaluated in conjugation with the coordinated dispatched of the stored energy of the water tank. Generator rescheduling is also deployed using predictive control action in [12]-[14]. The authors in [15] and [16] used rescheduling in congestion management in addition to line overload mitigation.

Dynamic security comprises transient security and voltage security. Dynamic security dispatch or control action is also a necessary step that is taken after any creditable contingency. Dynamic security is threatened during the loss of generation and other situations. In [17], the authors designed an intelligent system by radial function based on a neural network, and the proposed methodology is tested on the IEEE-50 bus system. In [18], bender decomposition-based optimization with security constraint function is employed and the proposed methodology is applied to the IEEE-114 bus system.

The main objective of this paper is to develop a single integrated control scheme for control in a corrective state. This paper proposes a control strategy based on the nonlinear dynamic theory that can automatically handle the generation setpoint depending on the post-contingency scenario. For a system with a large number of machines and buses, it is difficult to derive a control scheme based on analytical methods due to the presence of variables. Therefore, this paper incorporates a nonlinear stability theory for developing control schemes with measurable variables as input for the control tasks. The search and optimization are inherent in the form of semidefinite programming. The central research gap that this paper addresses and fills is as below:

- There is very less attention to emergency security problems in the recent state-of-the-art literature.
- There is only an analytical optimization-based solution approach that cannot include the operational effects of AVR, AGC, and PSS that has no executive verification and gives a void solution for real-time.
- There is a lack of adequate control schemes incorporating the security dispatch problem under the energy management system.
- Various methodologies use a preexisting model of load frequency control so they cannot handle the case of area outage.

The key features of the proposed scheme are:

- It develops a ubiquitous method of generator rescheduling in the emergency security state of the power system.
- It can handle all types of contingency due to active power imbalance and utilizes an online measurement-based model configuration approach.
- It deploys advanced nonlinear control theory in the power system arena.
- It simplifies and solves all the optimization with all constraints by single linear matrix inequality.

## III. MATHEMATICAL MODELLING

According to the rotor dynamics equation

$$M\frac{d\omega}{dt} = p_{mi} - p_{ei} \tag{1}$$

where $M$ is angular momentum, $\omega$ is angular speed, $p_{mi}$ is the power input to the rotor, and $p_{ei}$ is power developed by the electromagnetic reaction which is given as

$$p_{ei} = E'_{qi}\left[\sum\nolimits_{j=1}^{j=n} E'_{qj}(B_{ij}\sin\delta_{ij} + G_{ij}\cos\delta_{ij})\right] \tag{2}$$

where $E'_{qi}$ is quadrature axis sub transient voltage, $B_{ij}$ is an element of reduced susceptance matrices reduced bus, $G_{ij}$ is conductance element of reduced bus matrices, and $\delta_{ij}$ is angle difference between buses.

On substitution (2) in (1) and replacing $M$ by $\frac{H_i}{\pi f}$, angular acceleration is given by

$$\frac{d\omega}{dt} = \left(-E'_{qi}\left[\sum\nolimits_{j=1}^{j=n} E'_{qj}(B_{ij}\sin\delta_{ij} + G_{ij}\cos\delta_{ij})\right] + p_{me}\right)\Big/\frac{H_i}{\pi f} \tag{3}$$

This can be rewritten as

$$\frac{d\omega}{dt} = \left(-E'_{qi}\left[\sum\nolimits_{j=1}^{j=n} E'_{qj}G_{ij}\cos\delta_{ij}\right] + p_{me}\right)\Big/\frac{H_i}{\pi f} \tag{4}$$

where,

$$\dot{E'_{qi}} = \left[-E_{qi} + E_{fi}\right]/T_{doi} \tag{5}$$

where $E_{fi}$ is rotor field voltage to produce per unit voltage at generator terminal, and $T_{doi}$ is direct axis open-circuit time constant of the rotor in (6)–(8), as shown at the bottom of the next page.

Manipulating (8) can be further reduced to

$$\dot{E'_{qi}} = \left[-E'_{qi} + \left(x_{di} - x'_{di}\right)\sum\nolimits_{j=1}^{j=n} E'_{qj}B_{ij}\right]\Big/T_{doi} + E_{fi}/T_{doi} \tag{9}$$

Now, expanding (4) for the $N$ machine system, the system represented by (5), (6), and (7) is represented in (10) and (11), as shown at the bottom of the next page.

## IV. KRASOVSKII's THEOREM FOR NON-ZERO EQUILIBRIUM POINT

Let the system be defined by $f(x)$ where $x \in \mathbb{R}^n$ has dynamics equation described by

$$\begin{aligned} \dot{x_1} &= f^1\left(x_1, x_2, x_3, x_4, x_5, \ldots\ldots\ldots x_n\right) \\ f(x) = \dot{x_2} &= f^2\left(x_1, x_2, x_3, x_4, x_5, \ldots\ldots\ldots x_n\right) \\ &\vdots \\ \dot{x_n} &= f^n\left(x_1, x_2, x_3, x_4, x_5, \ldots\ldots\ldots x_n\right) \end{aligned} \tag{12}$$

$$\hat{F} = \tilde{F} + \tilde{F}^* \tag{13}$$

Equation (12) has an equilibrium point at $x_{n,} = 0$, where n $\in$ {1, 2, 3...n}, then $f(x)$ is asymptotically stable at its equilibrium point $x_{n,} = 0$ if matrices $\hat{F}$ given by (13) is a definite negative. Where $\tilde{F}$ is jacobian of $f(x)$ and is given as

$$\tilde{F} = J\left\{\begin{array}{c} f^1\left(x_1, x_2, x_3, x_4, x_5, \ldots\ldots\ldots x_n\right) \\ \vdots \\ f^n\left(x_1, x_2, x_3, x_4, x_5, \ldots\ldots\ldots x_n\right) \end{array}\right\} \tag{14}$$

$\tilde{F}^*$ is transpose of $\tilde{F}$, and is given as

$$\tilde{F} = \left\{\begin{array}{ccc} \frac{df^1}{dx_1} & \cdots & \frac{df^1}{dx_n} \\ \vdots & \ddots & \vdots \\ \frac{df^n}{dx_1} & \cdots & \frac{df^n}{dx_n} \end{array}\right\} \tag{15}$$

The system represented by equation (12) has the Lyapunov energy function of $\tilde{F}X\tilde{F}^*$.

Now let the dynamical system (12) has non-zero equilibrium points at $x_{n,} = x_n^{eq}$, where, where n $\in$ {1, 2, 3 ... n}, then (12) can be modified by change of variables with $X_n = x_n - x_n^{eq}$ as represented in (16).

$$\begin{aligned} \dot{X_1} &= f^1\left((X + x_1^{eq}), (X_2 + x_2^{eq}), \right. \\ &\qquad \left.\left(X_{3,} + x_3^{eq}\right), \ldots\ldots\ldots (X_n + x_n^{eq})\right) \\ \dot{X_2} &= f^2\left((X_1 + x_1^{eq}), (X_2 + x_2^{eq}), \right. \\ &\qquad \left.\left(X_{3,} + x_3^{eq}\right), \ldots\ldots\ldots (X_n + x_n^{eq})\right) \\ &\vdots \\ \dot{X_n} &= f^n\left((X_1 + x_1^{eq}), (X_2 + x_2^{eq}), \right. \\ &\qquad \left.\left(X_{3,} + x_3^{eq}\right), \ldots\ldots\ldots (X_n + x_n^{eq})\right) \end{aligned} \tag{16}$$

Now system represented by equation (16) has an equilibrium point of the modified variable with $\boldsymbol{X_i} = 0$, and the actual variable with $x_i, = x_i^{eq}$.

## V. PROBLEM FORMULATION AND SOLUTION METHODOLOGY

A multi-machine generator system that is interconnected with load and transmission lines has many variables and parameters associated with it. A speed governor and AVR accompany each generator for maintaining the supply at rated frequency and voltage. During contingencies, the speed and voltage

$$\dot{E'_{qi}} = \left[-\left(E'_{qi} + \left(x_{di} - x'_{di}\right) I_{di}\right) + E_{fi}\right] \Big/ T_{doi} \tag{6}$$

$$\dot{E'_{qi}} = \left[\begin{array}{c} -\left(E'_{qi} + \left(x_{di} - x'_{di}\right) \sum_{j=1}^{j=n} E'_{qj}(G_{ij} \sin \delta_{ij} - B_{ij} \cos \delta_{ij})\right) \\ +E_{fi} \end{array}\right] \Big/ T_{doi} \tag{7}$$

$$\dot{E'_{qi}} = \left[-\left(E'_{qi} + \left(x_{di} - x'_{di}\right) \sum_{j=1}^{j=n} E'_{qj}(G_{ij} \sin \delta_{ij} - B_{ij} \cos \delta_{ij})\right)\right] \Big/ T_{doi} + E_{fi} \Big/ T_{doi} \tag{8}$$

$$\left.\begin{array}{l} \frac{d\omega_1}{dt} = \left(\left[-(E'^{\,2}_{q1})G_{11} - E'_{q1}E'_{q2}G_{12} \cdots - E'_{q1}E'_{qn-1}G_{1n-1} - E'_{q1}E'_{qn}G_{in}\right] + p_{me1}\right) \Big/ \frac{H_1}{\pi f} \\ \frac{d\omega_2}{dt} = \left(\left[-E'_{q2}E'_{q1}G_{21} - \left(E'^{\,2}_{q2}\right) G_{22} \cdots - E'_{q2}E'_{qn-1}G_{2n-1} - E'_{q2}E'_{qn}G_{2n}\right] + p_{me2}\right) \Big/ \frac{H_2}{\pi f} \\ \qquad\qquad \vdots \\ \frac{d\omega_n}{dt} = \left(\left[-E'_{qn}E'_{q1}G_{n1} - E'_{qn}E'_{q2}G_{n2} \cdots - E'_{qn}E'_{qn-1}G_{nn-1} - (E'^{\,2}_{qn})G_{nn}\right] + p_{men}\right) \Big/ \frac{H_n}{\pi f} \end{array}\right\} \tag{10}$$

$$\left.\begin{array}{l} \dot{E'_{q1}} = \left[-E'_{q1} + \left(x_{d1} - x'_{d1}\right) E'_{q1}B_{11} + \left(x_{d1} - x'_{d1}\right) E'_{q2}B_{12} + \ldots \left(x_{d1} - x'_{d1}\right) E'_{qn}B_{1n}\right] \Big/ T_{do1} + E_{f1} \Big/ T_{do1} \\ \dot{E'_{q2}} = \left[\left(x_{d2} - x'_{d2}\right) E'_{q2}B_{21} + -E'_{q2} + \left(x_{d2} - x'_{d2}\right) E'_{q2}B_{22} + \ldots \left(x_{d2} - x'_{d2}\right) E'_{qn}B_{2n}\right] \Big/ T_{do2} + E_{f2} \Big/ T_{do2} \\ \qquad\qquad \vdots \\ \dot{E'_{qn}} = \left[\left(x_{dn} - x'_{dn}\right) E'_{qn}B_{n1} + \left(x_{dn} - x'_{dn}\right) E'_{qn}B_{2n} + \ldots - E'_{qn} + \left(x_{dn} - x'_{dn}\right) E'_{qn}B_{nn}\right] \Big/ T_{don} + E_{fn} \Big/ T_{don} \end{array}\right\} \tag{11}$$

of the generator deviate from the rated value, and various parameters like an admittance of the network are altered. The control scheme should bring all crucial variables like voltage and frequency to their normal rated ones as they were in the pre-contingency situations. Now taking a step for rotor angular transient stability for the multi-machine system, we consider the system represented by (10) and (11). Now under steady-state, i.e. before any contingency, $E'_{qn} = E'^{STEADY}_{qn}$ and $\omega_n = 1$ respectively, in per-unit, where n $\in \{1, 2, 3 \ldots n\}$.

Inclusion of AGC: the AGC consists of a speed governor, turbine, value link, and joints. The $P_{mei}$ term in equation (10) is the power delivered to the generator through turbine input. In this paper, the speed governor and turbine model is not taken in the equation model due to its complex linear and nonlinear characteristics, but in the simulation environment all these things are taken and $P_{mei}$ is as input for the set point of the turbine.

The equation (10) represents the interrelation between the field exciter current and quadrature axis sub-transient voltage where $E_{fi}$ is input to AVR reference input.

Now, after contingency, it has to bring all the state values i.e. $E'_{qn}$ and $\omega_n$ back to steady-state pre-contingency values. The dynamical system represented by (10) and (11) is a nonlinear system with a non-zero equilibrium point. For deploying the control scheme according to (16), the variables are substituted in a below-described manner.

Let $\omega_n - 1 = X_n$, so $X_n = 0 \Leftrightarrow \omega_n = 1$. Again $E'_{qn} - E'^{STEADY}_{qn} = Y_n$ and henceforth $Y_n = 0 \Leftrightarrow E'_{qn} = E'^{STEADY}_{qn}$, so by substituting the variable of the target system (10) and (11) as $\omega_n = X_n + 1$, $E'_{qa} = Y_n + E'^{STEADY}_{qn}$. Here the reader should keep in mind that variable $X_{i+1} \forall i \geq 1 and \leq 2n$ can be interchangeable with variable $Y_i \forall i \geq 1 and \leq n$ here $X_{2n} \in \mathbb{R}^{2n}$ or $X_{2n} \in \left\{\omega_1, \omega_2, \ldots \omega_n, E'_{q1}, E'_{q2}, \ldots\ldots E'_{qn}\right\}$ and $x^{eq}_{2n} \in \{1, 1 \ldots\ldots to\ ntimes, E'^{STEADY}_{q1}, E'^{STEADY}_{q2} \ldots\ldots E'^{STEADY}_{qn}\}$. on substituting the variable, finally (17), as shown at the bottom of the next page, is obtained. The rotor speed dynamics of the $n$ machine system are described by (10) which is a nonlinear system of variables $X_1, X_2, X_{3,\ldots\ldots} X_n, Y_1, \ldots\ldots Y_n$ as shown by (17) in standard form. Here $G_{ij}$ and $E'^{STEADY}_{qn}$ are constants and calculations are done to find the solution for $p_{me}$, such that for every post contingency set of $G_{ij}$ the system remains stable.

The system represented by (17) can be written in standard form

$$\Psi = f(\xi, P_{me}, E_{fi})$$

where $\boldsymbol{\Psi}$ is a series of differential equations with state $\xi \in \mathbb{R}^{2n}$ and control inputs $P_{me}$ and $E_{fi} \in \mathbb{R}^n$ and $f(.)$ is continuous time-bounded mapping $[f(.) : f(.) \in \mathbb{R}^{2n} \times \mathbb{R}^n \times \mathbb{R}^n \rightarrow \mathbb{R}^{2n}]$ let $\boldsymbol{\Psi}$ have an equilibrium point at $\xi = [\alpha_1, \alpha_2, \ldots\ldots \alpha_n, \beta_1 \beta_2 \ldots \beta_n]$ due to contingency the manifold of the variable deviates from its equilibrium point. To bring the manifold towards its equilibrium point which is a non-zero value. Again according to krassovskii's theorem there is a condition that is given by (18). Means $\boldsymbol{\xi}$ comprises of $[X_i + 1, Y_i + E'^{STEADY}_{qi}] \forall i \geq 1 and \leq n$.

$$\begin{aligned} J\left(f\left(\xi, P_{me}, E_{fi}\right)\right) + J\left(f\left(\xi, P_{me}, E_{fi}\right)\right)^* &< 0 \\ 0 < P_{me} &< 1 \\ E_{fi} &= 1 \end{aligned} \quad (18)$$

For stability of system (16), the condition given in (13) is imposed. Since the dynamical system represented by (17) consists of $E'^{STEADY}_{q1}, E'^{STEADY}_{q2} \ldots\ldots and\ E'^{STEADY}_{qn}$, the available variable from measurements are terminal voltage and current of each generator $V_{ti}$ and $I_{ti}$, where $i \in \{1, 2, 3 \ldots n\}$. By applying the park's transform, d-q ( $V_{tqi}, I_{tdi}$) component of terminal voltage and current is obtained to determine the value of $E'^{STEADY}_{q1}, E'^{STEADY}_{q2} \ldots\ldots and\ E'^{STEADY}_{qn}$. The values obtained from measurement are substituted for the equation $V_{tqi} + x_{di} I_{di} = E'_{qi}$ before pre-contingency. For rotor stability of $n$ machine system, the input variables are $p_{me1}, p_{me2} \ldots\ldots and\ p_{men}$ that has to be determined. System (17) is quadratic which makes the control structure self-regulatory and eases the calculations. It takes the values of input $p_{me1}, p_{me2} \ldots\ldots and\ p_{men}$ as below:

$$\begin{aligned} p_{me1} &= k1(X_1 + 1)^2 \\ p_{me2} &= k2(X_2 + 1)^2 \\ &\cdot \\ &\cdot \\ &\cdot \\ p_{men} &= kn(X_n + 1)^2 \end{aligned}$$

And field excitation is to be taken as

$$\begin{aligned} E_{f1} &= K_1(X_n + 1)^2 = 1 \\ E_{f2} &= K_2(X_n + 1)^2 = 1 \\ &\cdot \\ &\cdot \\ E_{fn} &= K_n(X_n + 1)^2. = 1 \end{aligned}$$

On taking Jacobian operation and summation of its transpose as by (13) and (14) on the system (17), it becomes a linear matrices inequality. The matrix contains the term $X_1, X_2 \ldots X_n, Y_1 Y_2 \ldots Y_n\ and\ k_1, k_2 \ldots k_n$. Finally the value of $X_1, X_2 \ldots X_n, Y_1 Y_2 \ldots Y_n$ is substituted by measurements value by slight algebraic operation in post contingency scenario that is $\omega_n - 1 = X_n$ and $E'_{qn} - E'^{STEADY}_{qn} = Y_n$. The final problem reduces to LMI of variables $k_1, k_2 \ldots k_n$ that is solved by CVX programming setup on MATLAB®. Figure-1 shows the flowchart of the proposed algorithm.

## VI. DEPLOYMENT OF PROPOSED ALGORITHM AND CASE STUDY

The proposed automatic self-regulatory control scheme for generator rescheduling is performed on the IEEE-10 Machine 39-bus system, also known as the New England System in

**TABLE 1. Description of values considered in simulation.**

| | |
|---|---|
| Low pass filter time constant (sec) | 0.01 |
| Regulator gain | 200 |
| regulator time constant (sec) | 0.015 |
| Lead-lag compensator time constant (sec) | 10 |
| Lead-lag compensator time constant (sec) | 1 |
| Terminal voltage (p.u) | 1.03 |
| Lower limit for regulator output | -5 |
| Upper limit for regulator output | 5 |

**TABLE 2. Configuration of all machines.**

| | |
|---|---|
| Global gain | 1 |
| Frequency of low-frequency band (Hz) | 0.2 |
| Gain of low-frequency band | 30 |
| Frequency of intermediate frequency band (Hz) | 1.25 |
| Gain of the intermediate frequency band | 40 |
| Frequency of high-frequency band (Hz) | 12 |
| Gain of high-frequency band | 160 |

MATLAB®/Simulink. The mentioned system has 10 generators, 39 interconnecting buses, and 19 loads. An AVR, speed governor, and power system stabilizer with standard parameters accompany each generator. All machines use IEEE Type-1 synchronous machine voltage regulator combined with an exciter.

The description of the system and the AVR data used in the simulation are summarized in Table-1.

The applied power system stabilizer is a multi-band PSS with simplified settings. All machines use multi-band PSS with configuration as summarized in Table-2.

The turbine used in the simulation is of a tandem compound single mass. All the configurations of speed governor and turbine used for all generators are summarized in Table-3.

The total generation capacity of this plant is 61408 MW, and loads connected to the network are 60963 MW. The initial setpoint of generators numbering from 1-10 is [1 .277 .65.63 .508 .650 .560 .540.830 .25]. The total margin between generation and load is 445 MW. Various contingency conditions considered and executed are as follows:

A. Single Load Outage
B. Multiple Load Outage

$$
\left.\begin{aligned}
\frac{dX_1}{dt} &= \left(\begin{bmatrix} -\left(\left(\left(Y_1 + E'^{STEADY}_{q1}\right)\right)^2\right) G_{11} - \left(Y_1 + E'^{STEADY}_{q1}\right)\left(Y_2 + E'^{STEADY}_{q2}\right) G_{12} \cdots \\ -\left(Y_1 + E'^{STEADY}_{q1}\right)\left(Y_{n-1} + E'^{STEADY}_{qn-1}\right) G_{1n-1} - \left(Y_1 + E'^{STEADY}_{q1}\right)\left(Y_n + E'^{STEADY}_{qn}\right) G_{in} \end{bmatrix} + p_{me}\right) \Big/ \frac{H_1}{\pi f} \\
\frac{dX_2}{dt} &= \left(\begin{bmatrix} -\left(Y_2 + E'^{STEADY}_{q2}\right)\left(Y_1 + E'^{STEADY}_{q1}\right) G_{21} - \left(\left(\left(Y_2 + E'^{STEADY}_{q2}\right)\right)^2\right) G_{22} \cdots \\ -\left(Y_2 + E'^{STEADY}_{q2}\right)\left(Y_n + E'^{STEADY}_{qn-1}\right) G_{2n-1} - \left(Y_2 + E'^{STEADY}_{q2}\right)\left(Y_n + E'^{STEADY}_{qn}\right) G_{2n} \end{bmatrix} + p_{me}\right) \Big/ \frac{H_2}{\pi f} \\
&\vdots \\
\frac{dX_n}{dt} &= \left(\begin{bmatrix} -\left(Y_n + E'^{STEADY}_{qn}\right)\left(Y_1 + E'^{STEADY}_{q1}\right) G_{n1} - \left(Y_n + E'^{STEADY}_{qn}\right)\left(Y_2 + E'^{STEADY}_{q2}\right) G_{n2} \cdots \\ -\left(Y_n + E'^{STEADY}_{qn}\right)\left(Y_{n-1} + E'^{STEADY}_{qn-1}\right) G_{nn-1} - (\left(\left(\left(Y_n + E'^{STEADY}_{qn}\right)\right)^2\right) G_{nn} \end{bmatrix} + p_{me}\right) \Big/ \frac{H_n}{\pi f} \\
\frac{dY_1}{dt} &= \left[\begin{bmatrix} -\left(Y_1 + E'^{STEADY}_{q1}\right) + \left(x_{d1} - x'_{d1}\right)\left(Y_1 + E'^{STEADY}_{q1}\right) B_{11} + \\ \left(x_{d1} - x'_{d1}\right)\left(Y_2 + E'^{STEADY}_{q2}\right) B_{12} \\ + \ldots \left(x_{d1} - x'_{d1}\right)\left(Y_N + E'^{STEADY}_{qN}\right) B_{1n} \end{bmatrix} \Big/ T_{do1} + E_{f1}/T_{do1}\right] \\
\frac{dY_2}{dt} &= \left[\begin{bmatrix} \left(x_{d2} - x'_{d2}\right)\left(Y_2 + E'^{STEADY}_{q2}\right) B_{21} - \left(Y_2 + E'^{STEADY}_{q2}\right) \\ \left(x_{d2} - x'_{d2}\right)\left(Y_2 + E'^{STEADY}_{q2}\right) B_{22} \\ + \ldots \left(x_{d2} - x'_{d2}\right)\left(Y_N + E'^{STEADY}_{qN}\right) B_{2n} \end{bmatrix} \Big/ T_{do2} + E_{f2}/T_{do2}\right] \\
&\vdots \\
\frac{dY_N}{dt} &= \left[\begin{bmatrix} \left(x_{dN} - x'_{dN}\right)\left(Y_N + E'^{STEADY}_{qN}\right) B_{N1} \\ + \left(x_{dN} - x'_{dN}\right)\left(Y_N + E'^{STEADY}_{qN}\right) B_{N2} \\ + \ldots \left(Y_N + E'^{STEADY}_{qN}\right) B_{NN} + \left(x_{d2} - x'_{d2}\right)\left(Y_N + E'^{STEADY}_{qN}\right) B_{2n} \end{bmatrix} \Big/ T_{doN} + E_{fN}/T_{doN}\right]
\end{aligned}\right\} \tag{17}
$$

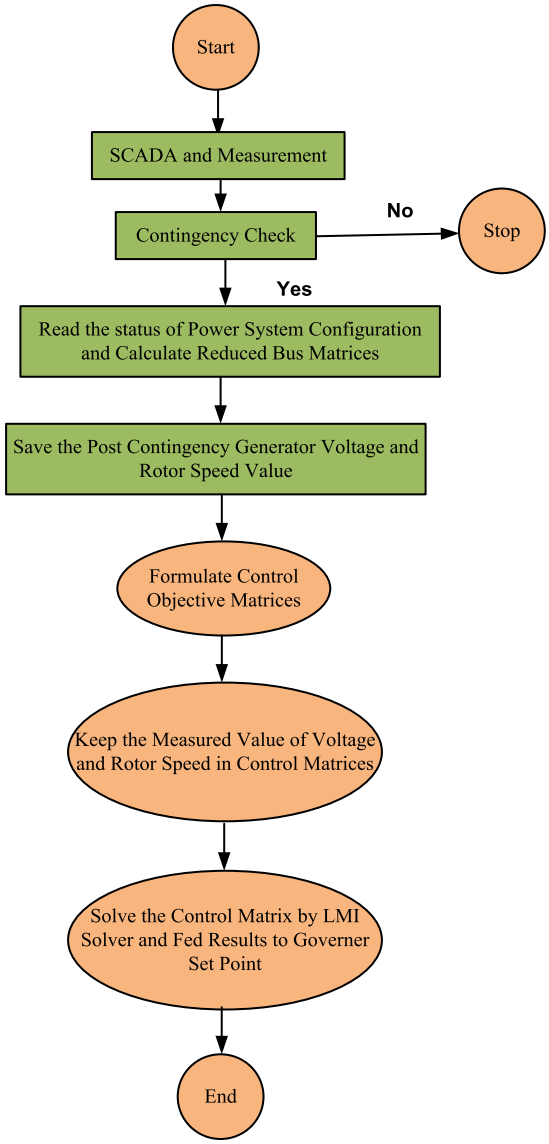


**FIGURE 1.** Flowchart of the proposed methodology.

**TABLE 3.** Configuration of speed governor and turbine.

| | |
|---|---|
| The gain, permanent droop (pu), and dead-zone width (pu) | [1 0.05 0] |
| The speed relay and gate servomotor time constants (s) | [0.001 0.15] |
| The turbine time constants T2 to T5 (s) | [0 10 3.3 0.5 ] |
| The turbine torque fractions F2 to F5. | [ 0 0.36 0.36 0.28 ] |

C. Area Outage
D. Load Increment

### A. SINGLE LOAD OUTAGE

The test system is simulated from the initial set value of the speed governor for 50 seconds. At the 5$^{th}$ second load at bus #39 with a load value of 1000 MW is removed permanently. All the rotor speed and terminal voltage of the generator are observed, as shown in Figure-3. Generator rescheduling program is performed and then after at 5.2$^{th}$ second new obtained value is feed to speed governor set point, the new rotor speeds are shown in Figure-4. The new set values calculated by the proposed method for generator #1-10 is as [0.5004 0.4988 0.4990 0.4986 0.4985 0.4989 0.4985 0.4985 0.4989 0.4994].

### B. MULTIPLE LOAD REMOVAL

Here, in this case, the load at buses#26, 28, and 29 are removed permanently at the 5$^{th}$ second during the simulation of 50 sec with an initial set value. Again the rescheduling is calculated and applied at a time 5.2$^{th}$ seconds. Generator rotor speed behavior is observed and plotted. The new set value calculated by the proposed method for generator #1-10 is [0.4999 0.4989 0.4991 0.4990 0.4987 0.4993 0.4988 0.4991 0.5008 0.4999]. Figure-5 and Figure-6 show the rotor speed before and after generator rescheduling, respectively.

### C. AREA OUTAGE

Figure-7 shows IEEE 39 bus network with area blackout (region hidden in Figure-7). In this case, the sectional area shown in black color suffers from blackout. This blackout area consists of generator #1 at bus #39 and generator #2 at bus #31 along with the loads at buses #39, 3, 4, 7, 8, and 31. The remaining area is in operational mode. The area shown in the figure goes to complete blackout at the 5$^{th}$ second of simulation. The blackout area is separated from the system at buses #3, and 6, and interconnecting lines between buses #1 and 39. Since the blackout area has loads greater than the generated power amount. So the remaining operating area has generation power greater than the available load. The new set value calculated by the proposed method for generator #3-10 is [0.5022 0.5004 0.4995 0.5005 0.5001 0.5005 0.5000 0.5018].

### D. LOAD INCREMENT

At the 5$^{th}$ second of simulation, in this case, loads connected to bus #18 are increased from 158 MW to 258 MW in active power. The load connected to bus #4 is increased from 400 MW to 500MW, and the load connected to bus #15 is increased from 320MW to 420MW. The total increment in load is 300 MW. The plant's total generating capacity is 61408 MW, and total loads increased to 61263 MW. New rescheduling of generator is fed to governor set point at the time the 5.2$^{th}$ second of the simulation. The new set value calculated by the proposed method for generator #1-10 is [1 0.6003 0.6001 0.6004 0.6006 0.6001 0.6006 0.6007 0.6002 0.5999].

## VII. DISCUSSION ON RESULTS

This paper proposes a generator rescheduling control strategy scheme. The proposed scheme is autonomous and self-regulatory by controlling the mechanical power of the governor by state feedback, like $p_{men} = kn(X_n + 1^2)$, where

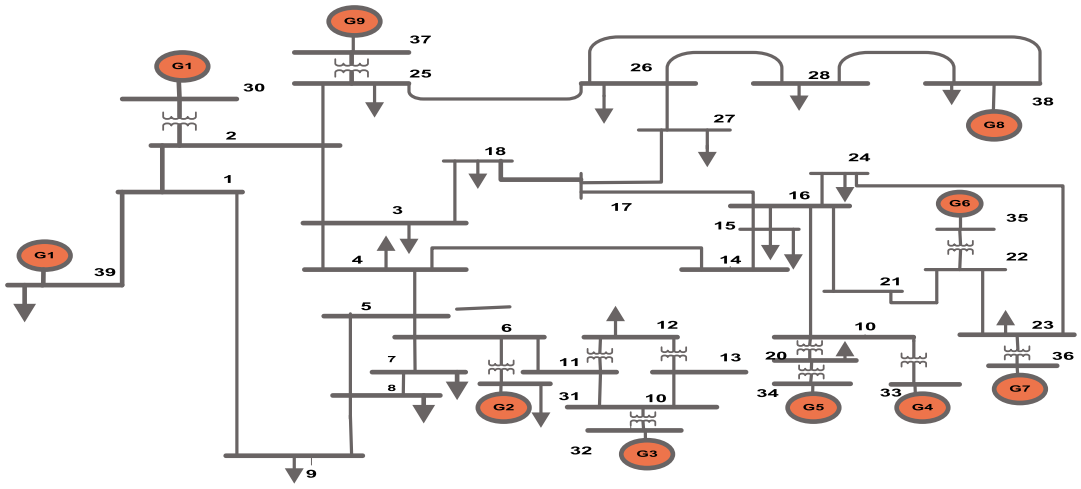


**FIGURE 2.** IEEE 10 Machine 39 bus system.

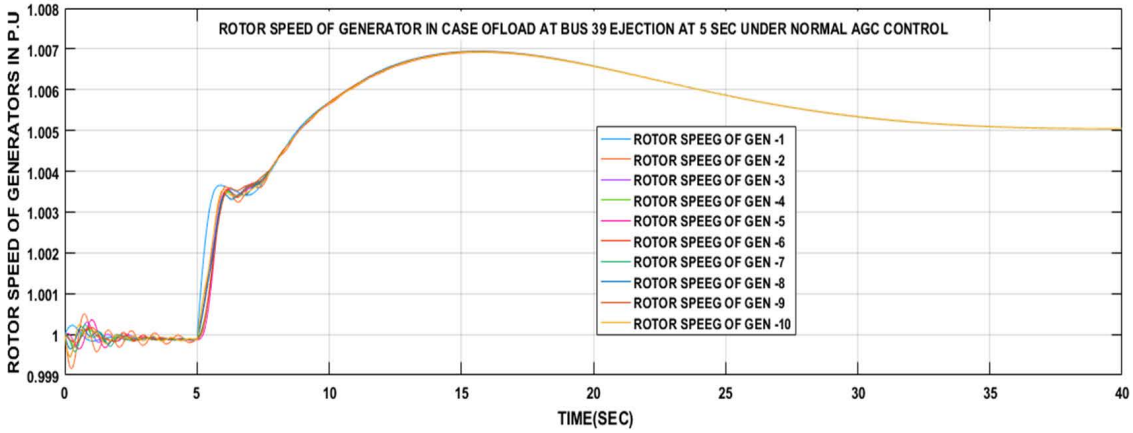


**FIGURE 3.** Rotor speed of all generators with the initial set point for Case-A.

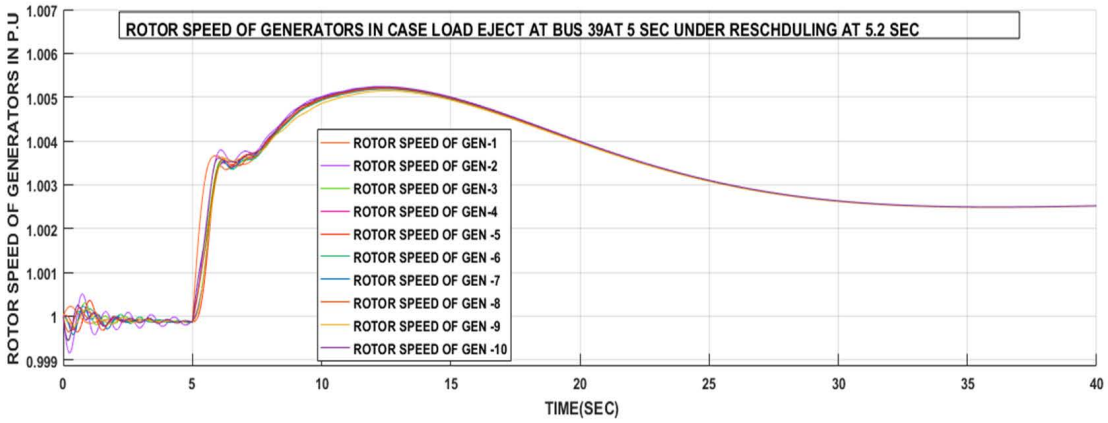


**FIGURE 4.** Rotor speed of all generators after rescheduling in Case-A.

$\omega_n - 1 = X_n$. Now since rotor speed is directly proportional to the frequency of generation, therefore, if loads decrease, the rotor speed increases, and vice versa. In these situations, the generator delivers power at a nonrated frequency that is harmful to the power transformer, electrical loads, and various power system accessories. Although the speed governor

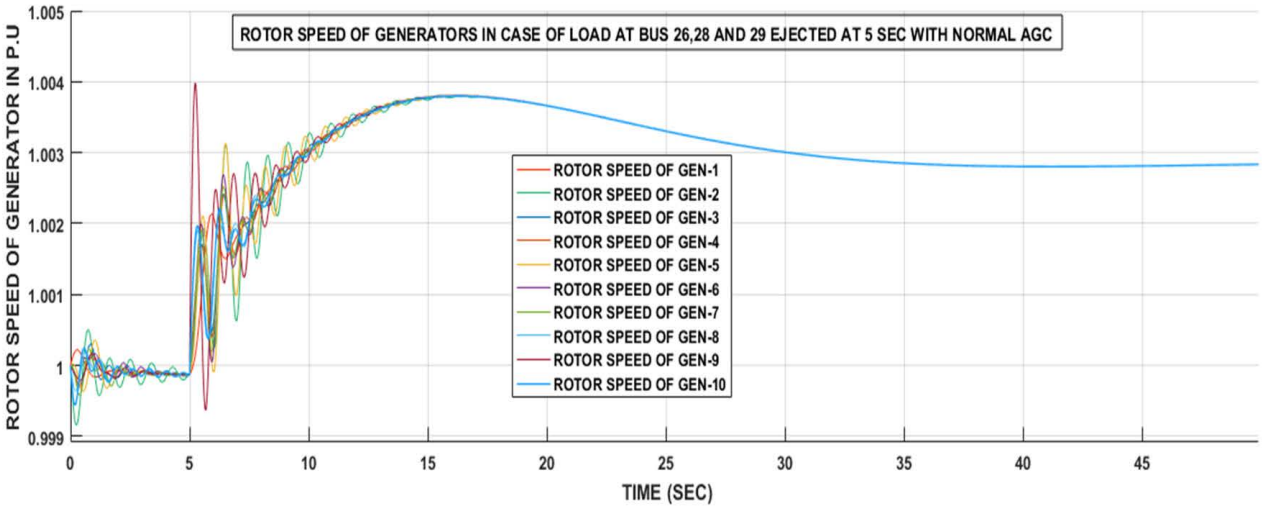


**FIGURE 5.** The rotor speed of all generators with an initial set point for Case-B.

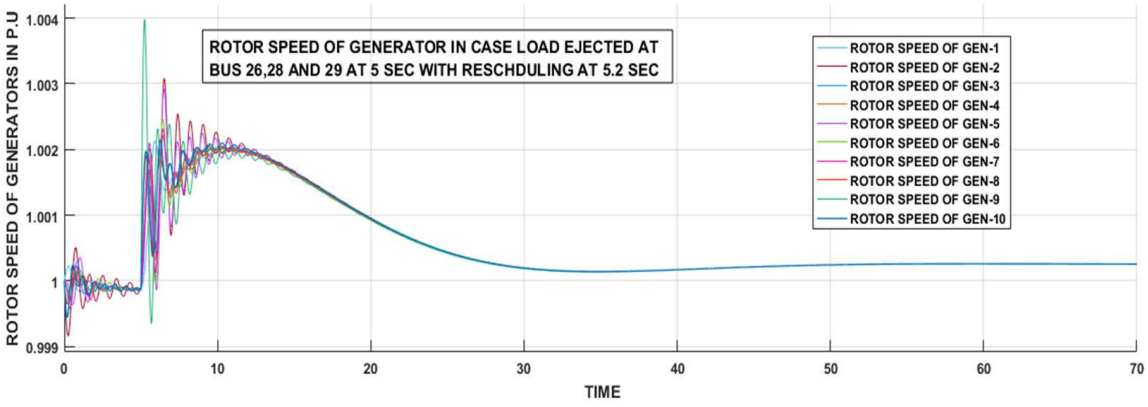


**FIGURE 6.** The rotor speed of all generators after rescheduling for Case-B.

of the generator performs the speed regulation of the rotor. Whilst in convention setup speed governor cannot prevent unnecessary power losses fed to the alternator. The solution proposed in this paper for generator rescheduling is performed when the active transfer capacity of the power system is greater than the demands. Now, speculating the results in this paper, the endpoint of rotor speed with an initial set point and proposed generator rescheduling are compared. The generator set points in different contingencies are summarized in Table-4.

Moreover, the rotor speed with the proposed methodology is closer to a steady-state value of 1 p.u. The power loss during the transient, i.e. $\sum_{i=1}^{i=n} \int (P_g - P_e)$ in different cases discussed are shown in Figures 12-15. It is observable that power loss by the proposed generator-rescheduling algorithm is very less than the convention setup except for Case #4. The power loss difference under Case #4 is only 45 MW. This minimum power loss for a bulk power system is negligible to attain rotor speed regulation. Figure 16 to 23 shows the governor set point variation for all four cases under normal and rescheduling. In Figures 16, 18, and 20 all governor's set points are decreasing up to sometime after contingency i.e. 5 sec. In Figure-22 governor set points are in an increasing

**TABLE 4.** Generator set points in different contingency discussed.

| Generator# | Initial | Case1 | Case2 | Case 3 | Case 4 |
|---|---|---|---|---|---|
| 1 | 1 | 0.5004 | 0.4999 | XXX | 1 |
| 2 | 0.277 | 0.4988 | 0.4989 | XXX | 0.6003 |
| 3 | 0.65 | 0.4990 | 0.4991 | 0.5022 | 0.6001 |
| 4 | 0.63 | 0.4986 | 0.4990 | 0.5004 | 0.6004 |
| 5 | 0.508 | 0.4985 | 0.4987 | 0.4995 | 0.6006 |
| 6 | 0.650 | 0.4989 | 0.4993 | 0.5005 | 0.6001 |
| 7 | 0.560 | 0.4985 | 0.4988 | 0.5001 | 0.6006 |
| 8 | 0.540 | 0.4985 | 0.4991 | 0.5005 | 0.6007 |
| 9 | 0.840 | 0.4989 | 0.5008 | 0.5000 | 0.6002 |
| 10 | 0.25 | 0.4994 | 0.4999 | 0.5018 | 0.5999 |

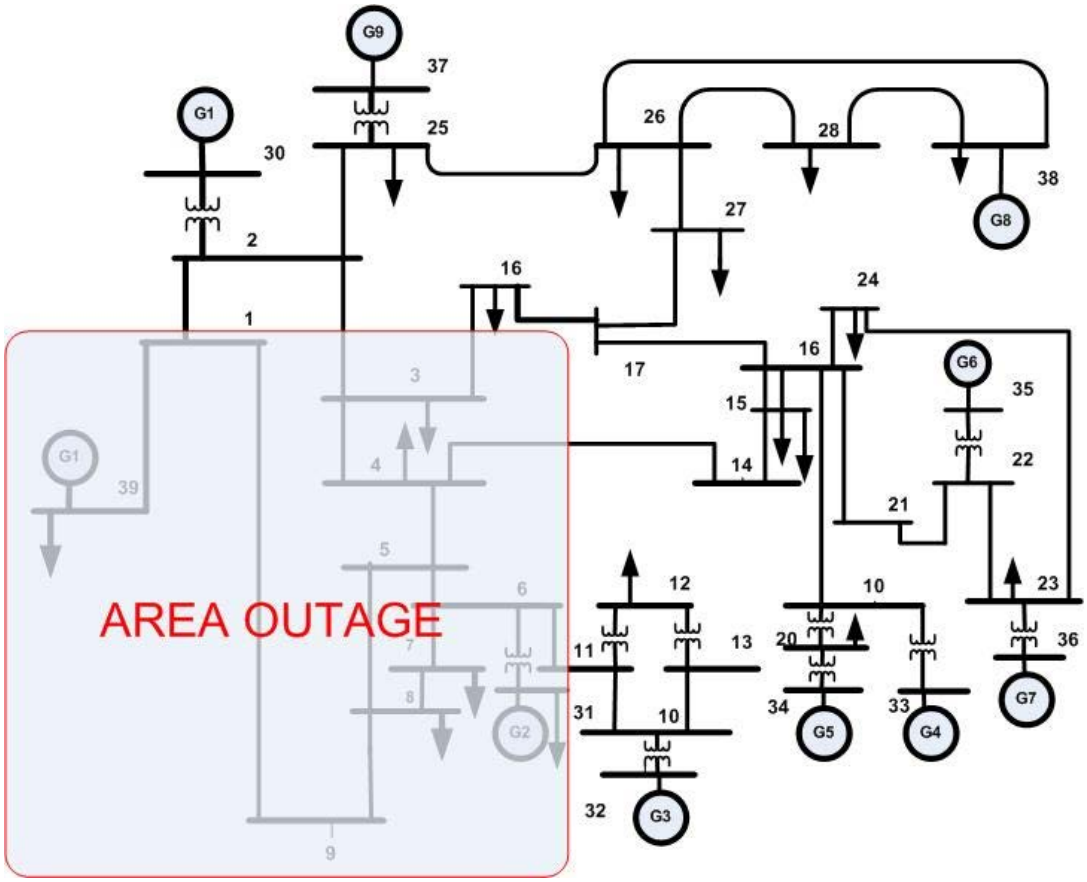


**FIGURE 7.** IEEE 39 bus system with area outage.

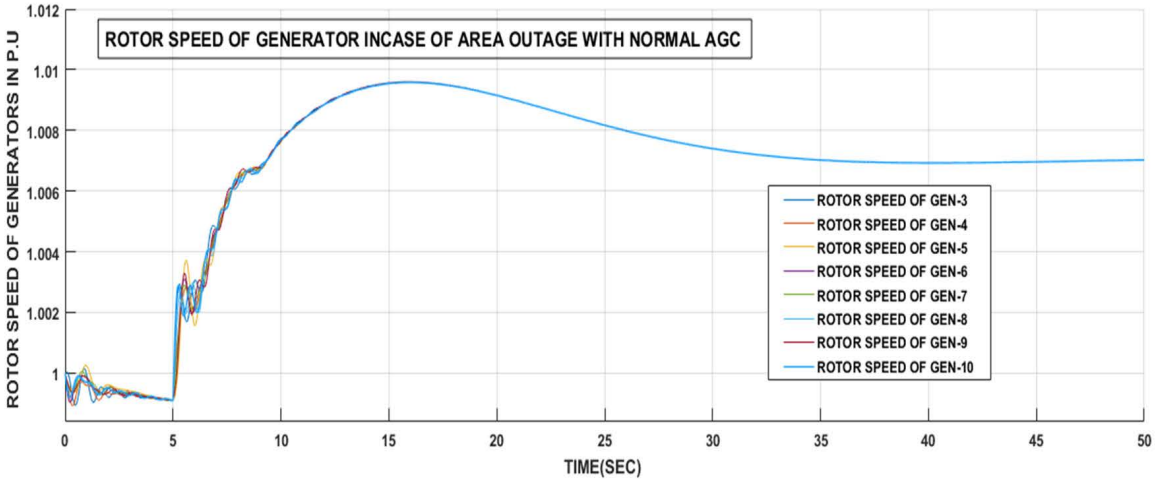


**FIGURE 8.** Rotor speed of all generators with the initial set point for Case-C.

and concave manner. Figures 16, 18, and 20 are cases #A, B, and C. In this case, power demands get reduced after contingency but in case #D the load demand increases more than the pre-contingency scenario. Figure 17, 19, 21, and 23 show the set point variation after rescheduling by the proposed methodology the governors' set point attaints its requested value gradually due to various time constant and valve action limit.

## VIII. DISCUSSION ON THE PERFORMANCES

The methodology proposed in this paper uses very few measurement network topologies in addition to the angular speed

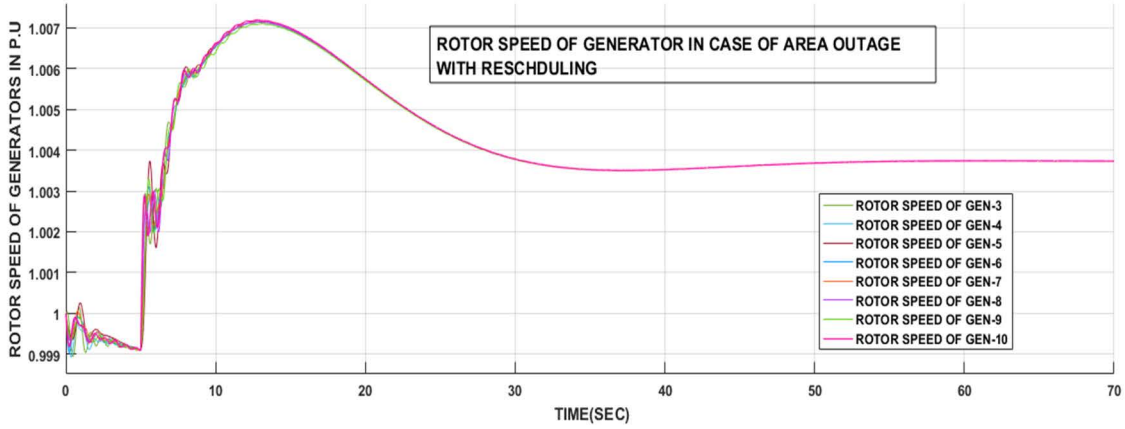


**FIGURE 9.** The rotor speed of all generators after rescheduling for Case-C.

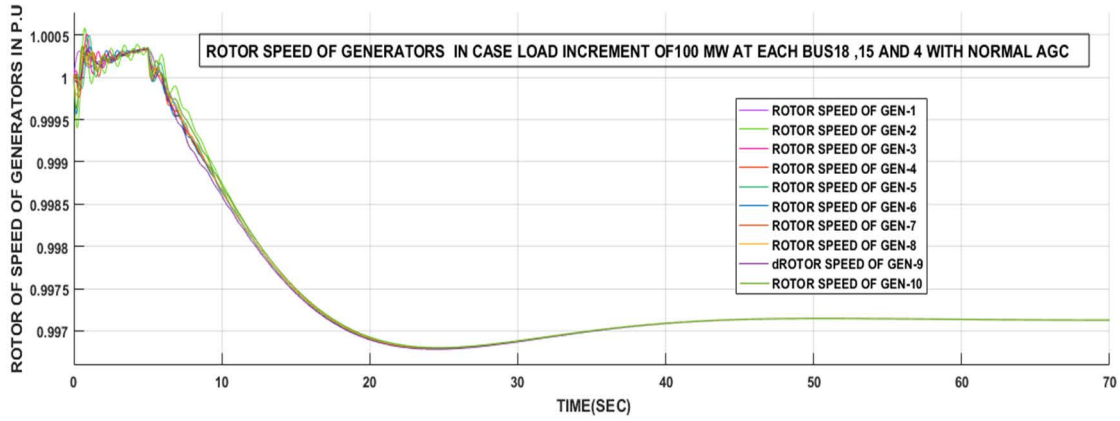


**FIGURE 10.** The rotor speed of all generators with an initial set point for Case-D.

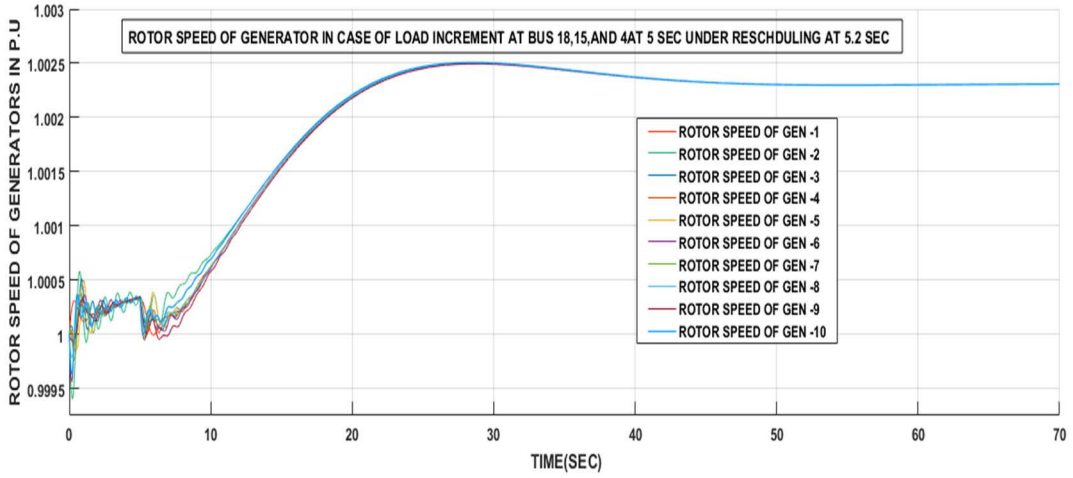


**FIGURE 11.** The rotor speed of all generators after rescheduling for Case-D.

of the generator, and the terminal voltage for the control objective formulation. As per (10) and (11) the system configured is of variable order depending on the measurements of loads and generator. It represents the existing and post-contingency system, which can handle area outages easily. Results reported in the paper also show that there is no

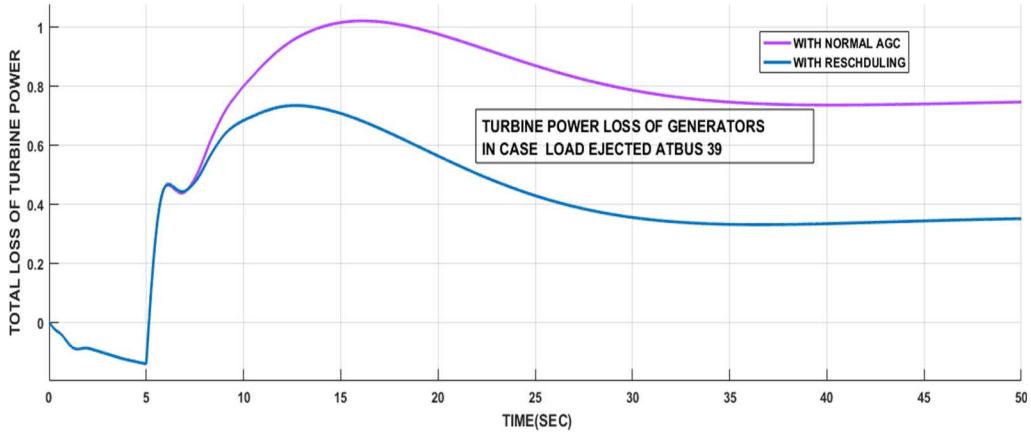


**FIGURE 12.** Energy loss of turbine output for Case #A.

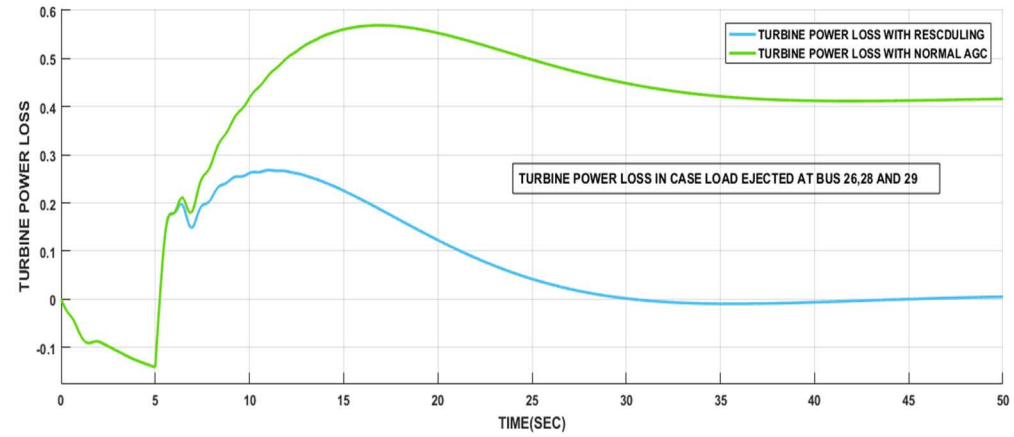


**FIGURE 13.** Energy loss of turbine output for Case #B.

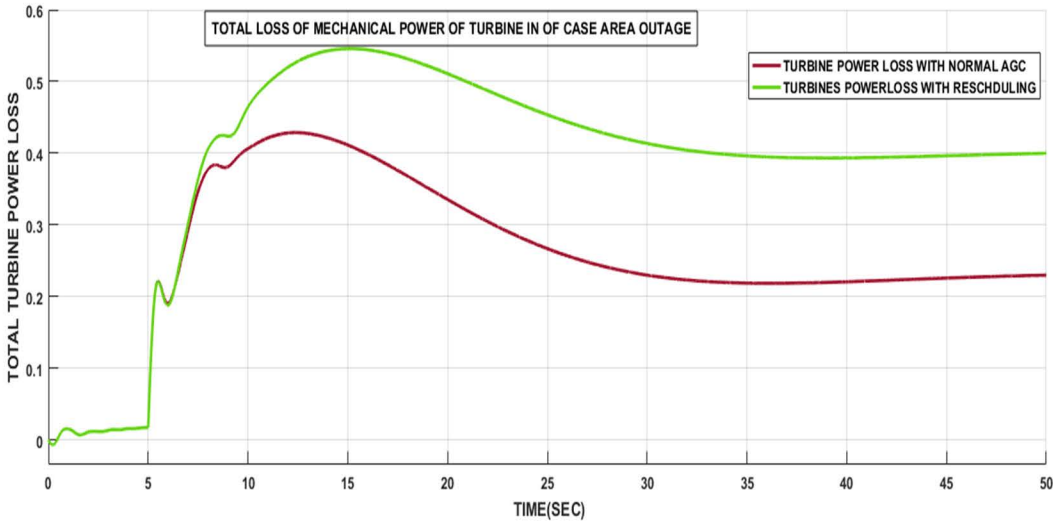


**FIGURE 14.** Energy loss of turbine output Case #C.

pre-existing model with a fixed parameter. The measurement taken to configure the system model is binary, i.e., line, load, and generator are either ON or OFF. So, in this regard, measurement noise also becomes uninterruptable for the system model configuration. The control input $P_{mei}$ and $E_{fi}$ is corresponding input to governor set value and AVR reference

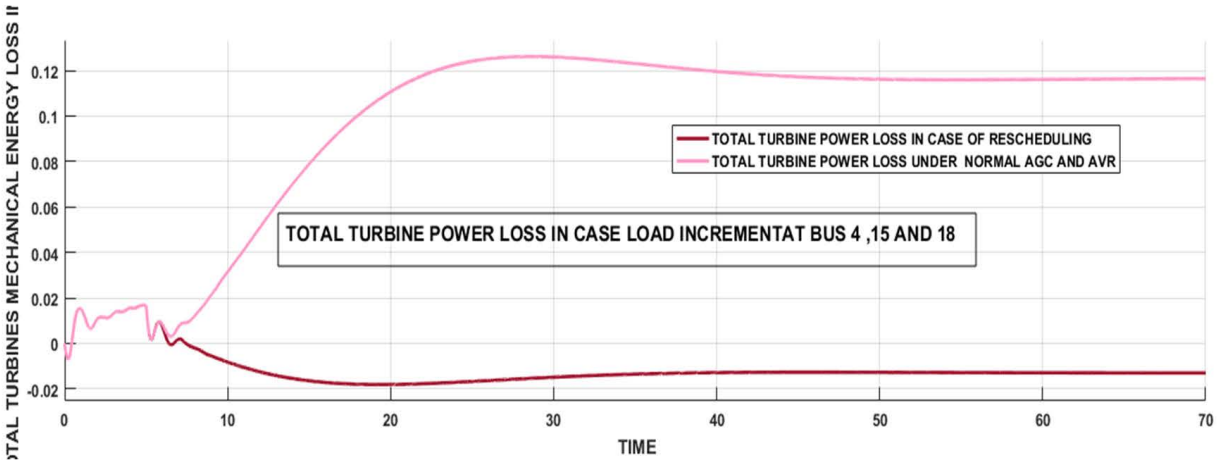


**FIGURE 15.** Energy loss of turbine output for Case #D.

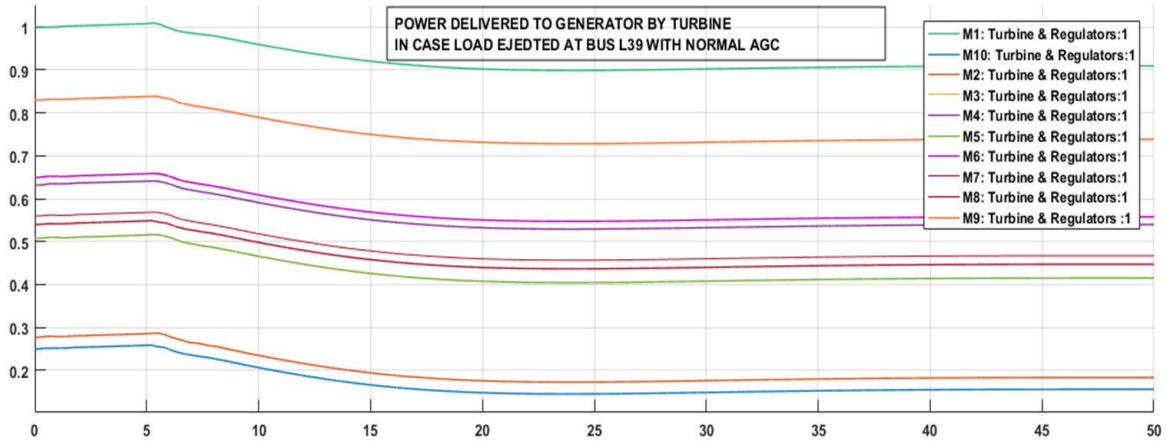


**FIGURE 16.** Governor set point variation in Case #A.

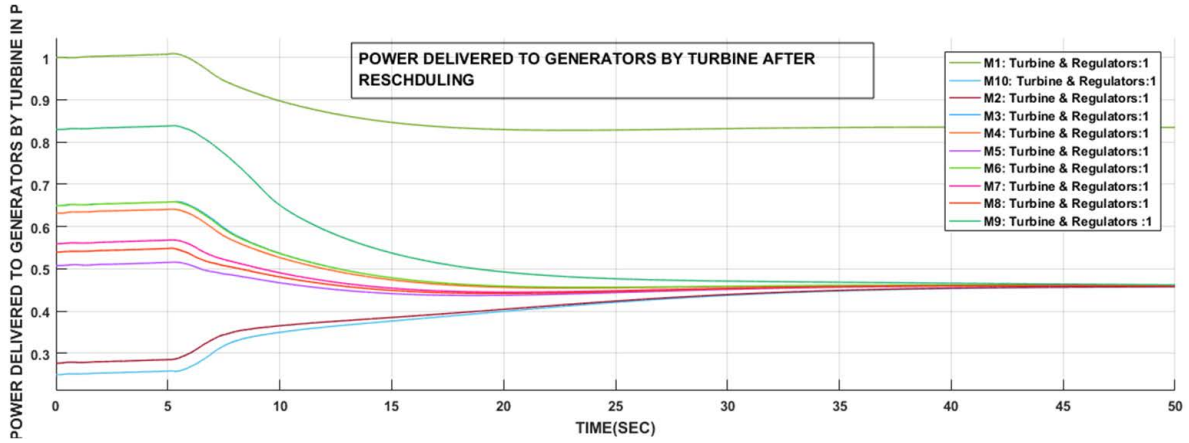


**FIGURE 17.** Governor set point variation with rescheduling in Case #A.

value. The whole problem to find the solution by (18) has inequality of $P_{mei} \leq 1$ and equality of $E_{fi} = 1$. Therefore, that control input is suitable not only during the transient period but also after the steady-state is achieved. A time gap between rescheduling and the contingency occurrence is taken as 0.2 seconds. So due to contingencies system

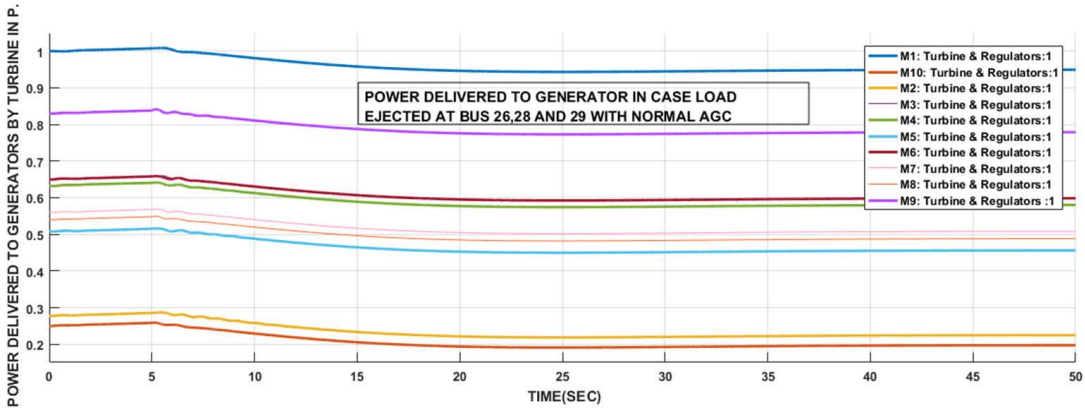


**FIGURE 18.** Governor set point variation in Case #B.

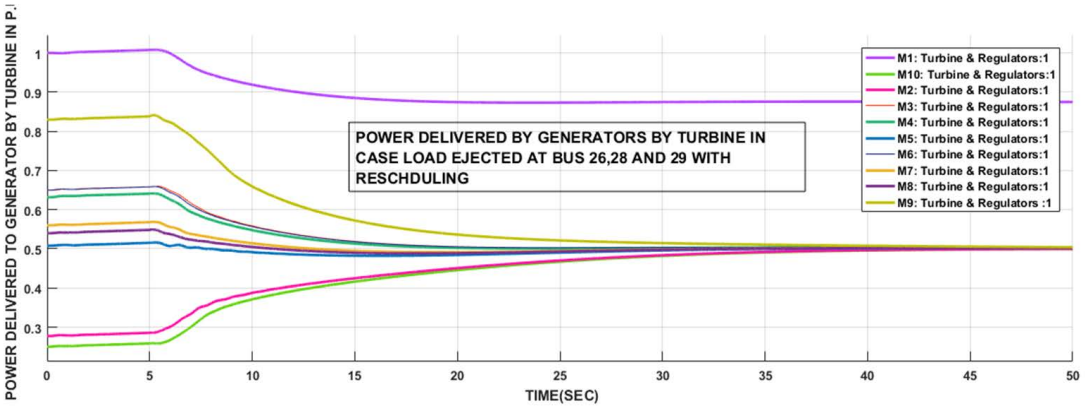


**FIGURE 19.** Governor set point with rescheduling variation in Case #B.

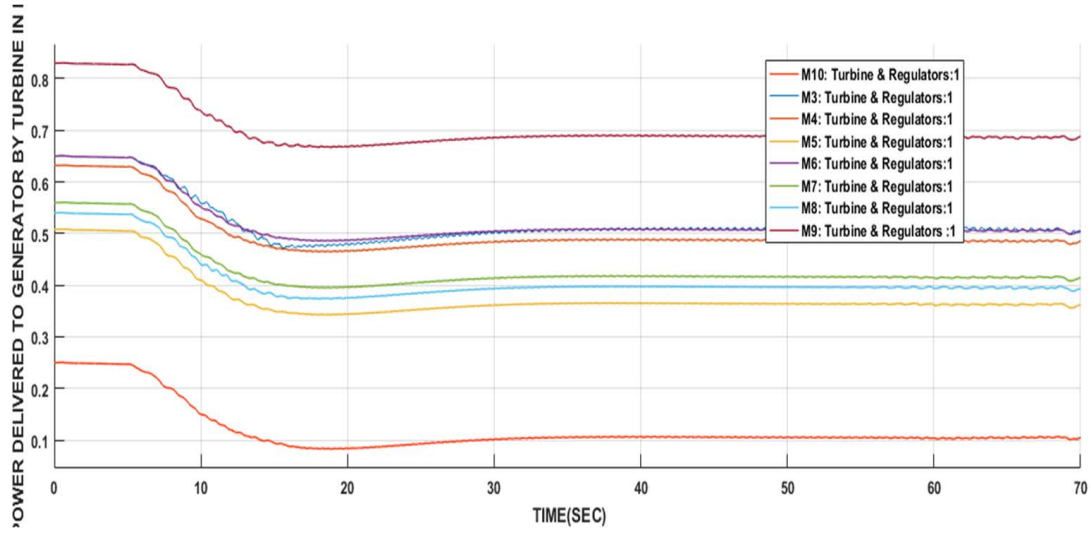


**FIGURE 20.** Governor set point variation in Case #C.

gets deviates from the equilibrium point. According to the Lyapunov theorem, the system should dissipative for stability criteria. So if the time gap between rescheduling and contingency is varied there is no effect on the stability of the system. According to (18) the corresponding solution always guaranteed a stable performance. In this paper, the

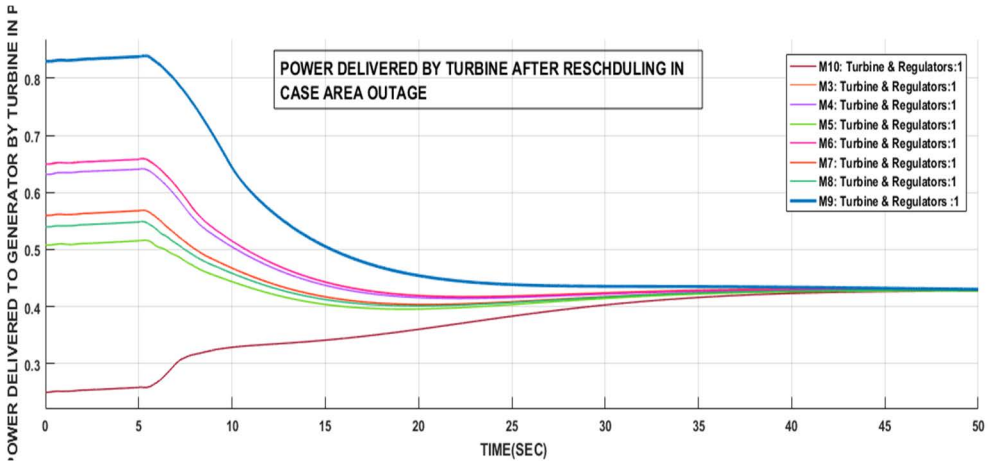


**FIGURE 21.** Governor set point-rescheduling variation in Case #C.

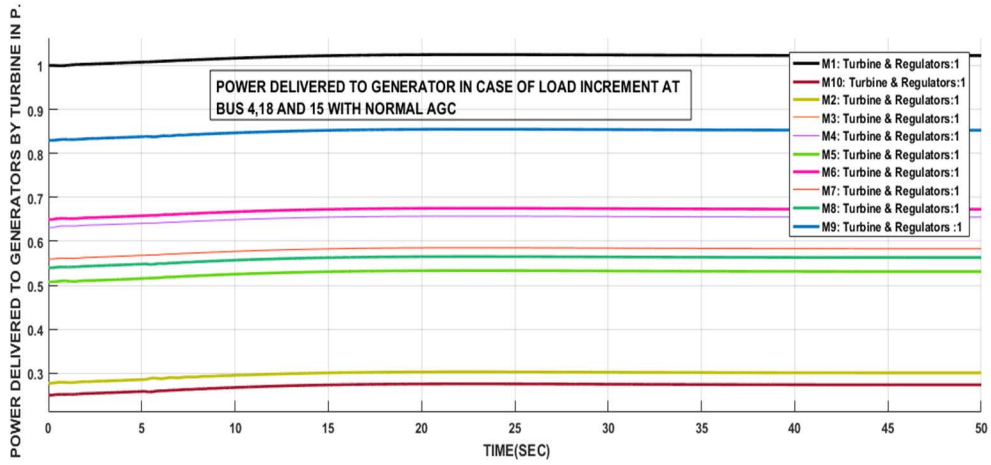


**FIGURE 22.** Governor set point variation in Case #D.

**TABLE 5.** Time taken to achieve the steady-state.

| Settling time | Case-A | Case-B | Case-C | Case-D |
|---|---|---|---|---|
| With normal AGC | 37 sec | 37 sec | 37 sec | 60 sec |
| With proposed rescheduling | 32 sec | 32 sec | 32 sec | 50 sec |

**TABLE 6.** Steady state value achieving in different cases.

| Steady state value of rotors Speed in p.u | Case-A | Case-B | Case-C | Case-D |
|---|---|---|---|---|
| With normal AGC | 1.005 | 1.0029 | 1.0068 | .9972 |
| With proposed rescheduling | 1.0025 | 1.0008 | 1.0035 | 1.0022 |

corresponding field excitation is always kept 1 after rescheduling, also there is no change in field excitation control and AVR performance, this is observed in Figures 24 to 27. In addition, the generator terminal voltage attains a steady-state value earlier in the rescheduling case.

**TABLE 7.** Power loss description in different contingency cases discussed.

| S.NO | Loss without generator rescheduling (P.U) | Loss with generator rescheduling (P.U) | Total energy saving in (MW) |
|---|---|---|---|
| Case #1 | 0.68 | 0.28 | 400 MW |
| Case #2 | 0.41 | 0 | 400 MW |
| Case #3 | 0.40 | 0.20 | 200 MW |
| Case #4 | 0.12 | -0.02 | 140 MW |

Table-8 presents a comparative assessment of performance obtained by the proposed scheme with that available in the literature.

The main findings of the paper are summarized as follows:

- The proposed rescheduling algorithm gives desired optimum results in all cases.

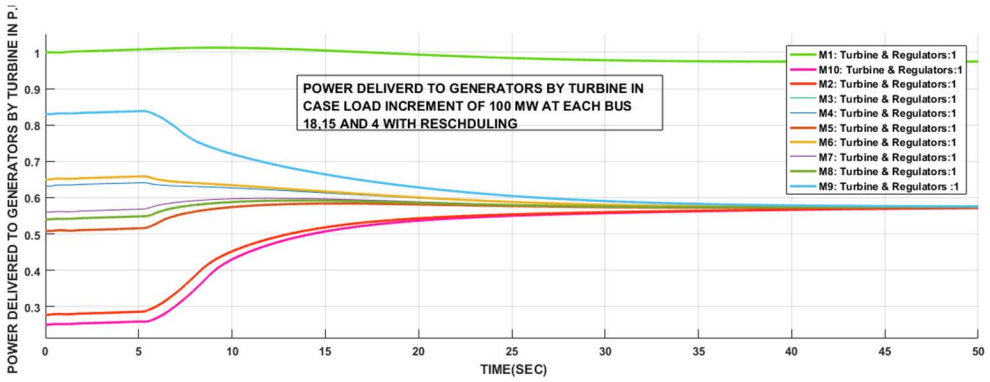


**FIGURE 23.** Governor set point variation with rescheduling in Case #D.

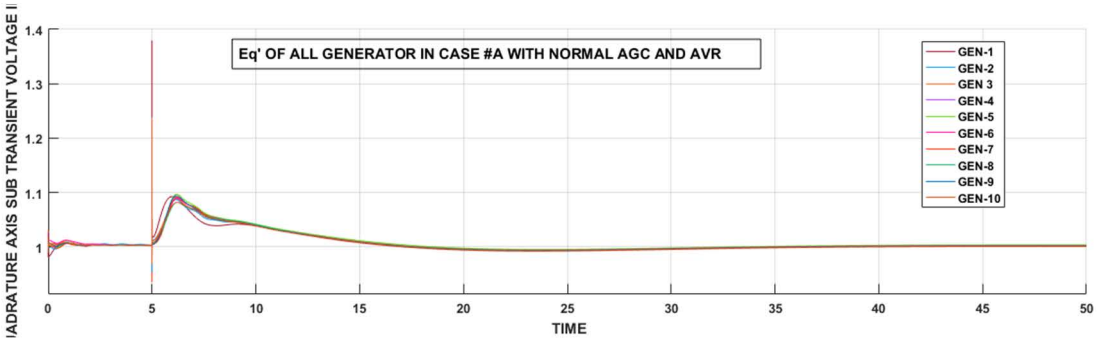


**FIGURE 24.** Terminal voltage of all buses in case #A with conventional AGC.

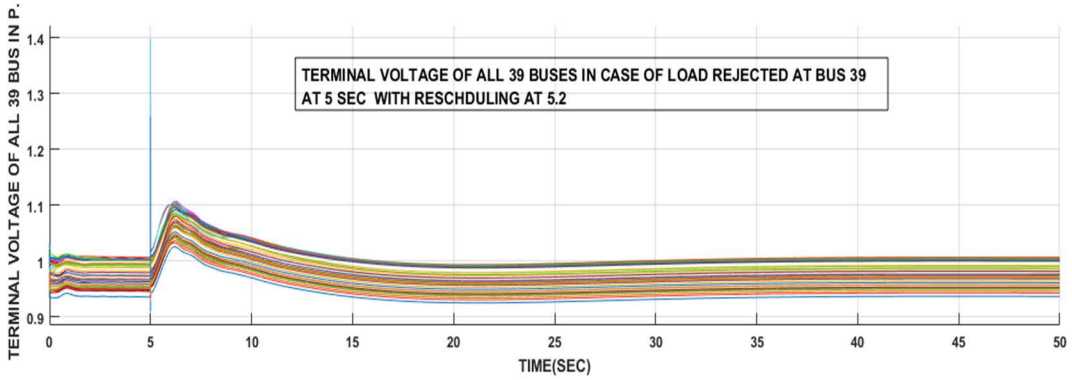


**FIGURE 25.** Terminal voltage of all buses after rescheduling in case #A.

**TABLE 8.** Comparative performance evaluation.

| Reference | AVR Consideration | AGC With Speed Governor Consideration | Area Outage Considered | Inter Oscillation Between Area | Single/Multiple Algorithm |
|---|---|---|---|---|---|
| [1] | No | Yes | No | Yes | Multiple |
| [6] | No | Yes | No | Yes | Single |
| [16] | Yes | No | No | Yes | Multiple |
| [18] | No | Yes | No | Yes | Single |
| Proposed Method | Yes | Yes | Yes | No | Single |

- The rescheduling set point of all generators tends to single value in all cases.
- There is less power loss by this methodology than the conventional speed governor performance.
- In case of load increment, the power loss is slightly more but the rotor speed settles to steady-state quickly.
- The inter rotor oscillation is negligible and rotors settle to steady-state quickly.

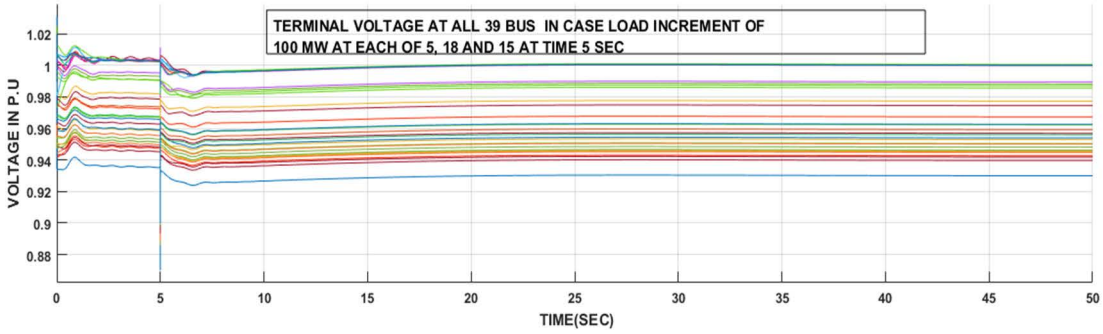


**FIGURE 26.** Terminal voltage of all buses in case #D with conventional AGC.

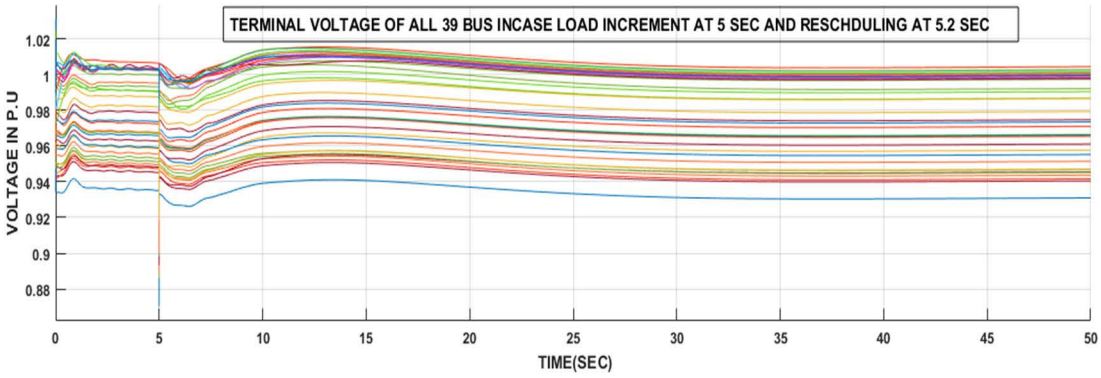


**FIGURE 27.** Terminal voltage of all buses after rescheduling in case #D.

## IX. CONCLUSION AND FUTURE SCOPE

In this paper, the IEEE 10-machine 39-bus system is considered with four conditional contingencies and a case study is done. In Case #A, a single load is removed, while in Case #B, multiple loads are removed, in Case #C, area blackout is considered and lastly, Case #D discusses the load increments at various buses is considered. The results of all the cases are classified into two categories. The first is with the initial setting of speed governors, and the second case is with the deployment of the proposed scheme after the implementation of rescheduling, according to the algorithm. The speed governor set point remains unaltered in each case of the first category. Every contingency is triggered at the $5^{th}$ second of the simulation. Rescheduling is implemented in all four cases at $5.2^{th}$ sec of the simulation and is carried out till steady state arrival. The results confirm that the settling time reduces to 5-10 sec, and steady-state rotor speed is near 1 under the rescheduling case. The mechanical power loss of all steam turbines that delivers power to the generator is reduced to 400 MW under a steady state. This power loss is prolonged and carried till the operation of the system It implies that the proposed rescheduling method is more efficient in energy saving. The economics of generation can also be fused into this ethology easily by incorporating the minimization objective function in (18). The generator rescheduling and load shedding for congestion mitigation based on the different cases of congestion mitigation and emergency stability can be performed by this proposed matrix by including the variable in $G_{ij}$ term in (10) and (11).

## REFERENCES

[1] X.-C. Shangguan, Y. He, C.-K. Zhang, L. Jin, W. Yao, L. Jiang, and M. Wu, "Control performance standards-oriented event-triggered load frequency control for power systems under limited communication bandwidth," *IEEE Trans. Control Syst. Technol.*, vol. 30, no. 2, pp. 860–868, Mar. 2022.

[2] H. Chávez, R. Baldick, and S. Sharma, "Governor rate-constrained OPF for primary frequency control adequacy," *IEEE Trans. Power Syst.*, vol. 29, no. 3, pp. 1473–1480, May 2014.

[3] O. Megel, T. Liu, D. J. Hill, and G. Andersson, "Distributed secondary frequency control algorithm considering storage efficiency," *IEEE Trans. Smart Grid*, vol. 9, no. 6, pp. 6214–6228, Nov. 2018.

[4] R. Patel, L. Meegahapola, L. Wang, X. Yu, and B. McGrath, "Automatic generation control of multi-area power system with network constraints and communication delays," *J. Modern Power Syst. Clean Energy*, vol. 8, no. 3, pp. 454–463, 2020.

[5] A. Sabo, N. I. A. Wahab, M. L. Othman, M. Z. A. B. M. Jaffar, H. Acikgoz, H. Nafisi, and H. Shahinzadeh, "Artificial intelligence-based power system stabilizers for frequency stability enhancement in multi-machine power systems," *IEEE Access*, vol. 9, pp. 166095–166116, 2021.

[6] X. Zhang, X. Zha, S. Yue, and Y. Chen, "A frequency regulation strategy for wind power based on limited over-speed de-loading curve partitioning," *IEEE Access*, vol. 6, pp. 22938–22951, 2018.

[7] T. Liu, W. Pan, R. Quan, and M. Liu, "A variable droop frequency control strategy for wind farms that considers optimal rotor kinetic energy," *IEEE Access*, vol. 7, pp. 68636–68645, 2019.

[8] D. H. Tungadio and Y. Sun, "Load frequency controllers considering renewable energy integration in power system," *Energy Rep.*, vol. 5, pp. 436–453, Nov. 2019.

[9] Y. Liu, Q. H. Wu, and X. X. Zhou, "Co-ordinated multiloop switching control of DFIG for resilience enhancement of wind power penetrated power systems," *IEEE Trans. Sustain. Energy*, vol. 7, no. 3, pp. 1089–1099, Jul. 2016.
[10] V. Veerasamy, N. I. A. Wahab, R. Ramachandran, M. L. Othman, H. Hizam, A. X. R. Irudayaraj, J. M. Guerrero, and J. S. Kumar, "A Hankel matrix based reduced order model for stability analysis of hybrid power system using PSO-GSA optimized cascade PI-PD controller for automatic load frequency control," *IEEE Access*, vol. 8, pp. 71422–71446, 2020.
[11] W. Pan, Z. Zhu, T. Liu, M. Liu, and W. Tian, "Optimal control for speed governing system of on-grid adjustable-speed pumped storage unit aimed at transient performance improvement," *IEEE Access*, vol. 9, pp. 40445–40457, 2021.
[12] M. Han, J. Fan, and J. Wang, "A dynamic feedforward neural network based on Gaussian particle swarm optimization and its application for predictive control," *IEEE Trans. Neural Netw.*, vol. 22, no. 9, pp. 1457–1468, Sep. 2011.
[13] F. Capitanescu, T. V. Cutsem, and L. Wehenkel, "Coupling optimization and dynamic simulation for preventive-corrective control of voltage instability," *IEEE Trans. Power Syst.*, vol. 24, no. 2, pp. 796–805, May 2009.
[14] H. Yuan and Y. Xu, "Trajectory sensitivity based preventive transient stability control of power systems against wind power variation," *Int. J. Electr. Power Energy Syst.*, vol. 117, May 2020, Art. no. 105713.
[15] S. S. Reddy, "Multi-objective based congestion management using generation rescheduling and load shedding," *IEEE Trans. Power Syst.*, vol. 32, no. 2, pp. 852–863, Mar. 2017.
[16] M. M. Esfahani and G. R. Yousefi, "Real time congestion management in power systems considering quasi-dynamic thermal rating and congestion clearing time," *IEEE Trans. Ind. Informat.*, vol. 12, no. 2, pp. 745–754, Apr. 2016.
[17] E. M. Voumvoulakis and N. D. Hatziargyriou, "A particle swarm optimization method for power system dynamic security control," *IEEE Trans. Power Syst.*, vol. 25, no. 2, pp. 1032–1041, May 2010.
[18] M. Ma and L. Fan, "Security constrained DC OPF considering generator responses," *Electric Power Syst. Res.*, vol. 192, Mar. 2021, Art. no. 106920.

**AMRENDRA KUMAR KARN** received the B.Tech. degree in electrical engineering from the Birsa Institute of Technology (formerly known as the Bihar Institute of Technology), Sindri, Dhanbad, Jharkhand, India, in 2011, and the M.Tech. degree in power system from the National Institute of Technology, Patna, Bihar, India, in 2016. He is currently pursuing the Ph.D. degree in control and instrumentation with Aligarh Muslim University, Uttar Pradesh, India. After his B.Tech. degree, he joined Tata Group Company Tata Robinson Fraser Jamshedpur as an Engineer and worked on various power plant erection and commissioning ongoing projects in India. He left his job for higher studies, in 2013. After completing his master's degree, he joined various engineering colleges as a Visiting Assistant Professor in Bihar. His research interests include advanced control, nonlinear control, fault tolerance, and robust control applications in the power system domain.

**SALMAN HAMEED** (Senior Member, IEEE) received the B.Sc. (Eng.) degree in electrical and the M.Sc. (Eng.) degree in power system and drives from the Department of Electrical Engineering, Aligarh Muslim University (AMU), Aligarh, in 1988 and 1991, respectively, and the Ph.D. degree in the area of power systems (FACTS controllers) from IIT Roorkee, in 2008. He is currently working as a Professor with the Department of Electrical Engineering, AMU. His teaching and research interests include power systems, applications of AI techniques in power systems, fuzzy logic controllers, and application of nanotechnology in solar PV cells. He is a Gold Medalist and a recipient of a University Merit Scholarship from AMU. He was a recipient of a QIP research fellowship from IIT Roorkee. He has delivered many invited talks at various institutes outside Aligarh. He has also chaired several technical sessions at international and national conferences, including a technical session held at Vancouver, Canada, in August 2014, International Conference on Power Systems Engineering (ICPSE 2014). He also visited Yokohama, Japan, to present a paper at IEEE Conference, in October 2002. He was a Member-Expert Committee for All India Council for Technical Education (AICTE), Central Regional Office, Bhopal, in 2011 and 2012. He has been the Advisor to UPSC, New Delhi. He is supervising three Ph.D. thesis right now and four Ph.D. thesis has been already supervised. He is a Life Member of System Society of India. He has published several research papers in national and international journals, such as *International Journal of Electrical Power and Energy Systems* (Elsevier), *Electric Power Systems Research* (Elsevier), and in various international and national conference proceedings in India and abroad. He is also the Chairman of the Electrical Engineering Department, AMU.

**MOHAMMAD SARFRAZ** (Member, IEEE) received the B.Tech. degree in electrical engineering from HBTI, Kanpur, in 2003, the master's degree in intelligent systems from the University of Sunderland, U.K., and the Ph.D. degree from the University of Salford, Manchester, U.K.

He is currently an Assistant Professor with the Department of Electrical Engineering, Aligarh Muslim University, Aligarh, and also associated with the Centre for Biomedical Engineering and the Centre for Artificial Intelligence, Faculty of Engineering & Technology. He is also the Deputy Coordinator at the Medical Device Monitoring Centre (MDMC) under Meteriovigilance Programme of India (MvPI), Ministry of Health and Family Welfare, Government of India. His teaching and research interests include in the area of instrumentation, smart systems, biomedical devices, and artificial intelligence. He is a Life Member of the Soft Computing Research Society, Indian Society for Technical Education, and System Society of India.

**MOHD RIZWAN KHALID** (Member, IEEE) received the Ph.D. degree in electrical engineering from the Department of Electrical Engineering, Aligarh Muslim University, Aligarh, India.

Previously, he was a Student Research Associate and the Project Engineer with the Indian Institute of Technology Kanpur, Kanpur, India. His research interests include power electronics, power quality, electric mobility, and xEVs charging infrastructure.

**JONG-SUK RO** (Senior Member, IEEE) received the B.S. degree in mechanical engineering from Hanyang University, Seoul, South Korea, in 2001, and the Ph.D. degree in electrical engineering from Seoul National University (SNU), Seoul, in 2008. In 2014, he was with the University of Bath, Bath, U.K., as an Academic Visitor. From 2013 to 2016, he worked with the Brain Korea 21 Plus, SNU, as a BK Assistant Professor. He conducted research with the Electrical Energy Conversion System Research Division, Korea Electrical Engineering and Science Research Institute, as a Researcher, in 2013. From 2012 to 2013, he was with the Brain Korea 21 Information Technology, SNU, as a Postdoctoral Fellow. He conducted research with the Research and Development Center, Samsung Electronics, as a Senior Engineer, from 2008 to 2012. He is currently an Associate Professor with the School of Electrical and Electronics Engineering and an Adjunct Professor with the Department of Intelligent Energy and Industry (BK4), Chung-Ang University, Seoul. His research interests include the analysis and optimal design of next-generation electrical machines using smart materials, such as an electromagnet, piezoelectric, and magnetic shape memory alloy.